

Hypochlorous acid-mediated generation of glycerophosphocholine from unsaturated plasmalogen glycerophosphocholine lipids

Jacqueline LeBig, Jürgen Schiller, Jürgen Arnhold, and Beate Fuchs¹

University of Leipzig, Medical Faculty, Institute of Medical Physics and Biophysics, Leipzig, Germany

Abstract The myeloperoxidase-derived metabolite hypochlorous acid (HOCl) promotes the selective cleavage of plasmalogens into chloro fatty aldehydes and 1-lysophosphatidylcholine (LPC). The subsequent conversion of the initially generated LPC was investigated in plasmalogen samples in dependence on the fatty acid residue in the *sn*-2 position by matrix-assisted laser desorption and ionization time-of-flight mass spectrometry and ³¹P NMR spectroscopy. Plasmalogens containing an oleic acid residue in the *sn*-2 position are converted by moderate amounts of HOCl primarily to 1-lyso-2-oleoyl-*sn*-glycero-3-phosphocholine and at increased HOCl concentrations to the corresponding chlorohydrin species. In contrast, plasmalogens containing highly unsaturated docosahexaenoic acid yield upon HOCl treatment 1-lyso-2-docosahexaenoyl-glycerophosphocholine and glycerophosphocholine. The formation of the latter product denotes a novel pathway for the action of HOCl on plasmalogens.—LeBig, J., J. Schiller, J. Arnhold, and B. Fuchs. Hypochlorous acid-mediated generation of glycerophosphocholine from unsaturated plasmalogen glycerophosphocholine lipids. *J. Lipid Res.* 2007. 48: 1316–1324.

Supplementary key words ³¹P nuclear magnetic resonance • matrix-assisted laser desorption and ionization time-of-flight mass spectrometry • lysophosphatidylcholine

Olefinic residues of fatty acyl residues of phospholipids are an important target for oxidative damage induced by reactive oxygen species (ROS) known to occur under various pathological conditions, including chronic inflammation, atherosclerosis, aging, and cancer. Some mammalian tissues and cells, such as erythrocytes, kidney, lung, testes, skeletal muscle, brain, heart, and particularly selected animal spermatozoa (e.g., from bull), contain considerable levels of plasmalogen glycerophosphocholine lipids (1). Plasmalogens also represent an important target for ROS (2) and are often considered antioxidants. Although the 1-alkenyl residues in plasmalogens (mainly plasmalogen

glycerophosphocholine and glycerophosphoethanolamine) of mammalian cells are usually derived from saturated long-chain fatty aldehydes, the acyl residues are highly unsaturated (2). For instance, in spermatozoa from boar or bull, docosahexaenoic and docosapentaenoic acid residues do nearly occur exclusively (3). Accordingly, the oxidative attack of ROS may affect the vinyl-ether function as well as the olefinic residue in the fatty acid moiety (4). The presence of a vinyl-ether bond makes plasmalogens more susceptible to oxidative damages compared with their 1-acyl analogs (2). This has prompted the hypothesis that plasmalogens may act as ROS scavengers, protecting other phospholipids and lipoprotein particles from oxidative damage (2). Thus, plasmalogens seem to have an antioxidative effect toward many ROS (5).

Hypochlorous acid (HOCl) is generated by polymorphonuclear leukocytes under the catalysis of the enzyme myeloperoxidase (MPO) (6). HOCl reacts with a variety of molecules, including amino acids, proteins, carbohydrates, nucleic acids, and lipids (7–12). In the latter case, chlorohydrins are generated as the primary products when HOCl reacts with the double bonds in unsaturated phosphatidylcholines (12–14). HOCl and the MPO-H₂O₂-Cl⁻ system also induce the formation of 2-lysophosphatidylcholines (LPCs) in polyunsaturated phosphatidylcholines, as shown by matrix-assisted laser desorption and ionization time-of-flight mass spectrometry (MALDI-TOF MS) and ³¹P NMR spectroscopy (15, 16).

The vinyl-ether bond of plasmalogens is also assumed to represent the preferred target for reactive chlorinating

Abbreviations: 2-D-1-LPC, 1-lyso-2-docosahexaenoyl-*sn*-glycero-3-phosphocholine; GPC, glycerol-1-phosphocholine; HOCl, hypochlorous acid; LPC, lysophosphatidylcholine; 1-M-2-LPC, 1-myristoyl-2-lyso-*sn*-glycero-3-phosphocholine; 2-O-1-LPC, 1-lyso-2-oleoyl-*sn*-glycero-3-phosphocholine; OAPC_{plasm}, 1-*O*-1'-(*Z*)octadecenyl-2-arachidonoyl-*sn*-glycero-3-phosphocholine; ODPC_{plasm}, 1-*O*-1'-(*Z*)octadecenyl-2-docosahexaenoyl-*sn*-glycero-3-phosphocholine; OOPC_{plasm}, 1-*O*-1'-(*Z*)octadecenyl-2-oleoyl-*sn*-glycero-3-phosphocholine; MALDI-TOF MS, matrix-assisted laser desorption and ionization time-of-flight mass spectrometry; MPO, myeloperoxidase; PNA, *p*-nitroaniline; ROS, reactive oxygen species.

¹To whom correspondence should be addressed.

e-mail: beate.fuchs@medizin.uni-leipzig.de

Manuscript received 1 November 2006 and in revised form 6 February 2007.

Published, JLR Papers in Press, March 29, 2007.

DOI 10.1194/jlr.M600478-JLR200

species. It has been shown that the MPO-H₂O₂-Cl⁻ system promotes selective oxidative cleavage of the vinyl-ether bond of plasmalogens, liberating α -chloro fatty aldehydes and unsaturated 1-LPC (17, 18). α -Chloro fatty aldehydes at physiologically relevant concentrations induce neutrophil chemotaxis in vitro, suggesting that these compounds possess a role in neutrophil recruitment and signaling function (19). On the other hand, enhanced levels of LPC are known to be cytotoxic. Enhanced LPC formation induces membrane rupture, nuclear expansion, cell lysis, a sustained increase in intracellular Ca²⁺ levels, and the production of ROS with the consequence of cytotoxic injuries and necrosis (20). Because plasmalogen is preferentially oxidized in contrast to unsaturated phosphatidylcholine (21), the supposed protective action of plasmalogens as ROS scavengers could be in competition with the damaging effects of the oxidation products. An accumulation of α -chloro fatty aldehydes, including 2-chlorohexadecanal, has been found in activated neutrophils and monocytes as well as in infarcted myocardium and human atheromas (22). The selective oxidative cleavage of plasmalogens in human atherosclerotic lesions, leading to a novel population of unsaturated 1-LPCs, independent of the action of phospholipase A₂ (23), possesses proatherogenic properties (18, 24).

Here, we investigated the formation of HOCl-induced degradation products from unsaturated plasmalogen glycerophosphocholine lipids by MALDI-TOF MS and high-resolution ³¹P NMR spectroscopy. Effects on mono-unsaturated plasmalogen glycerophosphocholine and plasmalogen glycerophosphocholine esterified with docosahexaenoic acid in the *sn*-2 position of the glycerol backbone were compared. A novel effect of HOCl, the formation of glycerol-1-phosphocholine (GPC), was established.

MATERIALS AND METHODS

Chemicals

All chemicals for NMR spectroscopy (sodium cholate, EDTA, and deuterated water with an isotopic purity of 99.6%), buffer preparation (NaH₂PO₄·H₂O, Na₂HPO₄·2H₂O, and Tris), and matrix preparation [*p*-nitroaniline (PNA)] as well as all solvents (chloroform and methanol) and taurine were obtained in the highest commercially available purity from Fluka Feinchemikalien GmbH (Taufkirchen, Germany). 1-*O*-1'-Octadecenyl-2-docosahexaenyl-*sn*-glycero-3-phosphocholine (ODPC_{plasm}) and 1-*O*-1'-octadecenyl-2-oleoyl-*sn*-glycero-3-phosphocholine (OOPC_{plasm}) as well as the internal standards 1-myristoyl-2-lyso-*sn*-glycero-3-phosphocholine (1-M-2-LPC), POPC, and 1,2-dipalmitoyl-*sn*-glycero-3-phosphate were purchased from Avanti Polar Lipids (Alabaster, AL) as CHCl₃ solutions and used without further purification.

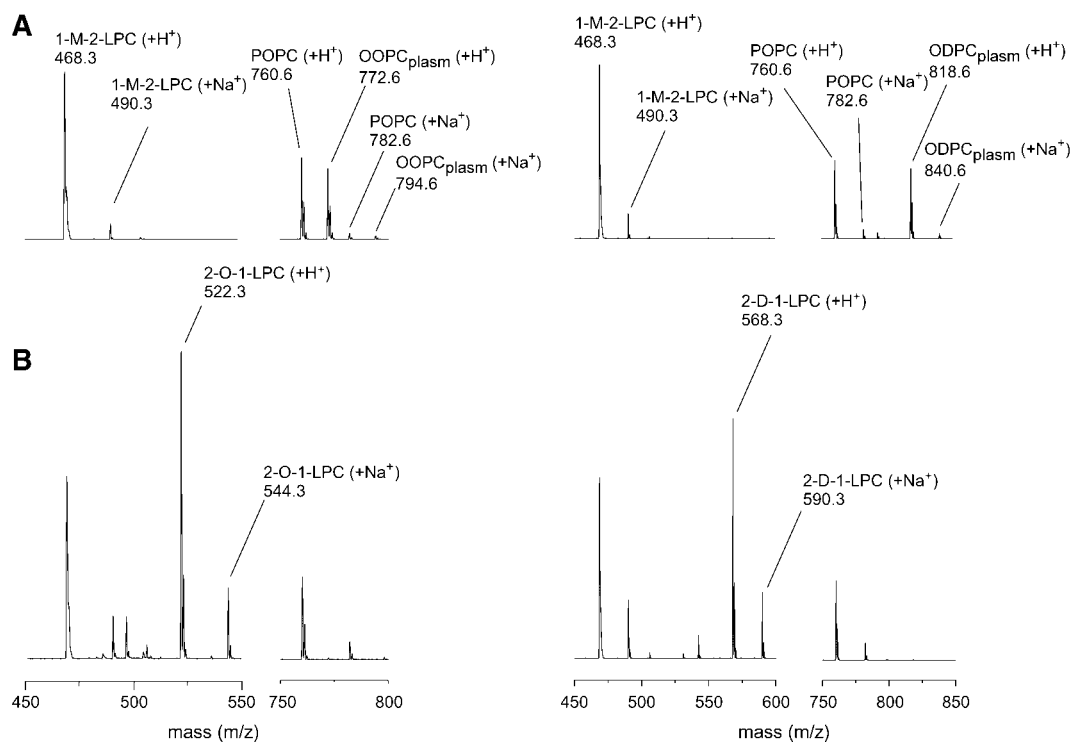


Fig. 1. Positive ion matrix-assisted laser desorption and ionization time-of-flight mass spectrometry (MALDI-TOF MS) mass spectra of the organic extracts of plasmalogen glycerophosphocholines after incubation with buffer (A) and 5 mM hypochlorous acid (HOCl) (B) for 1 h at room temperature. The HOCl incubation of 1-*O*-1'-(*Z*)octadecenyl-2-oleoyl-*sn*-glycero-3-phosphocholine (OOPC_{plasm}) is shown at left and that of 1-*O*-1'-(*Z*)octadecenyl-2-docosahexaenyl-*sn*-glycero-3-phosphocholine (ODPC_{plasm}) is shown at right. The plasmalogen concentration was 2 mM. The slight intensity differences between the H⁺ and Na⁺ adducts in the starting material and product spectra stem from the additional salt in the incubation buffer. Spectra were scaled according to the intensity of 1-myristoyl-2-lyso-*sn*-glycero-3-phosphocholine (1-M-2-LPC) standard, and the *m/z* values as well as peak assignments are indicated. 2-D-1-LPC, 1-lyso-2-docosahexaenyl-*sn*-glycero-3-phosphocholine; 2-O-1-LPC, 1-lyso-2-oleoyl-*sn*-glycero-3-phosphocholine.

HOCl incubation and lipid extraction

An aliquot of the corresponding plasmalogen glycerophosphocholine lipid dissolved in chloroform was evaporated to dryness. Multilamellar liposomes were prepared by dissolving the phospholipid film in 10 mM phosphate buffer (pH 7.4) and vortexing vigorously for 30 s. A stock solution of NaOCl was kept in the dark at 4°C. Its concentration was determined at pH 12 using $\epsilon_{290} = 350 \text{ M}^{-1} \text{ cm}^{-1}$ for ^-OCl (25). NaOCl was diluted with 10 mM phosphate buffer (pH 7.4) immediately before use. Liposomes (2 mM phospholipid) were incubated with varying concentrations of sodium hypochlorite for 1 h at pH 7.4. Adding an excess of taurine stopped the incubation. To extract the lipids, the same volume of a chloroform-methanol mixture (1:1, v/v) was added (26). Both the organic and the aqueous layers were used for further analysis.

MALDI-TOF MS measurements

Positive ion MALDI-TOF mass spectra were acquired on a Bruker Daltonics Autoflex workstation (Bremen, Germany). The system uses a pulsed nitrogen laser emitting at 337 nm. The extraction voltage was 20 kV, and 200 single laser shots were averaged for each mass spectrum. To enhance the spectral resolution, spectra were recorded in the reflector mode under "delayed extraction" conditions (27, 28). Internal standards were added for quantitative analysis (27–29). POPC and 1-M-2-LPC were added to the chloroform phase before MALDI-TOF MS. Furthermore, GPC amounts were estimated by comparison with the intensities of selected matrix peaks (28, 30). Organic or aqueous phases of the reaction extracts were applied to the MALDI target using PNA as the matrix (31). For the investigation of the organic and aqueous phases, the "low-mass gate" (matrix suppression) was set to m/z 315 and 150, respectively. All

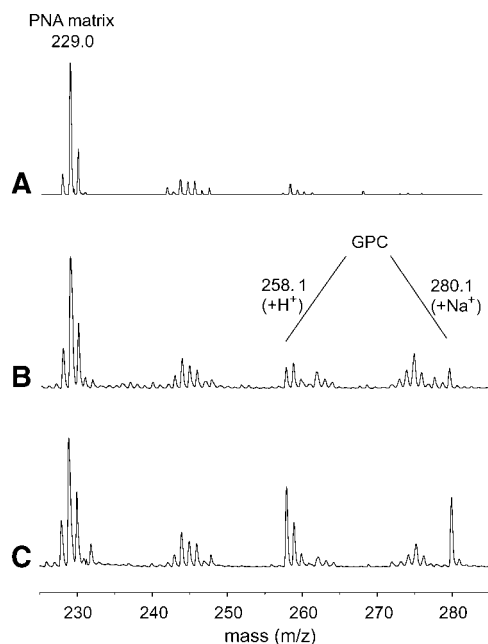


Fig. 2. Positive ion MALDI-TOF mass spectra of the aqueous extracts of plasmalogen glycerophosphocholines incubated with 10 mM HOCl for 1 h at room temperature. A: Laser desorption spectrum of the pure *p*-nitroaniline (PNA) matrix. B, C: Spectra of OOPC_{plasm} (B) and ODPC_{plasm} (C). Spectra were scaled according to the most intense matrix peak at m/z 229, and the m/z values as well as peak assignments are indicated. The same experimental parameters were used in all cases. GPC, glycerol-1-phosphocholine.

spectra were processed using the software Flex analysis version 2.2 provided by Bruker.

³¹P NMR spectroscopic measurements

The dried organic and aqueous layers were redissolved as described previously (32, 33) in 50 mM Tris (pH 7.65) containing 200 mM sodium cholate and 5 mM EDTA. As a concentration standard, 1,2-dipalmitoyl-*sn*-glycero-3-phosphate was added. After intense vortexing of the 0.5 ml samples, ³¹P NMR spectra were recorded in 5 mm NMR tubes on a Bruker DRX-600 spectrometer operating at 242.88 MHz for ³¹P. All measurements were performed using a direct "broad-band" NMR probe at 37°C and Waltz-16 composite pulse decoupling to eliminate ³¹P-¹H coupling. Pulse intervals of the order of T_1 permit the quantitative analysis of phosphorus resonance integral intensities (34).

Other NMR parameters were as follows: experiment time, 2–8 h; data size, 8 k; 60° pulse (7 μ s), pulse delay of 2 s; and line broadening of 1 Hz. Chemical shifts were referred to the most intense resonance of OOPC_{plasm} at $\delta = -0.60$ ppm and

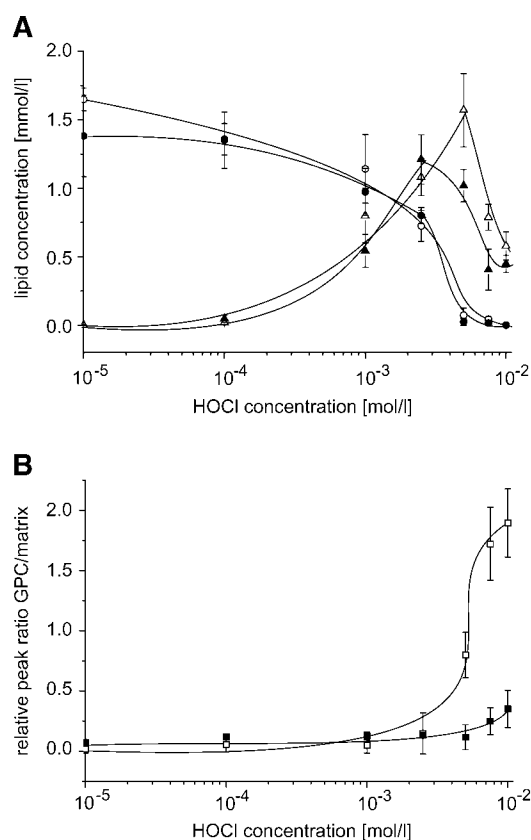


Fig. 3. Changes in the concentrations of ODPC_{plasm} (open circles), OOPC_{plasm} (closed circles), 2-D-1-LPC (open triangles), and 2-O-1-LPC (closed triangles) (A) as well as GPC derived from ODPC_{plasm} (open squares) and OOPC_{plasm} (closed squares) (B) as a function of HOCl concentration. Plasmalogens and 1-lyso-2-fatty acyl glycerophosphocholine lipids were determined from the peak intensities in the MALDI-TOF mass spectra with reference to the intensities of the peaks of POPC and 1-M-2-LPC used as standards (A). The sum of all individual adducts (H^+ and Na^+) was used as the intensity measure. In the case of GPC, the intensity ratio of the GPC peak at m/z 280.1 and the PNA matrix peak at 229.0 is indicated (B). Error bars represent SD of three independent measurements. The curved lines were not derived from a mathematical model but only represent spline curves to guide the eye.

ODPC_{plasm} at $\delta = -0.62$ ppm. All peak assignments were confirmed by comparison with the shift of commercially available reference compounds. Spectra were processed using the software 1D WIN-NMR version 6.2[®] (Bruker Analytische Messtechnik GmbH, Rheinstetten, Germany) including the deconvolution (II) routine for peak area determination.

RESULTS

Two selected plasmalogen glycerophosphocholines (ODPC_{plasm} and OOPC_{plasm}) were treated separately with increasing concentrations of HOCl. Plasmalogen species with oleoyl and docosahexaenoyl residues in the *sn*-2 position were chosen because significant differences in the yield of 2-LPC are known to occur when differently saturated diacyl-glycerophosphocholine lipids react with HOCl (15, 16). Selected examples of positive ion MALDI-TOF mass spectra of the organic phase of chloroform-methanol extracts of the reaction mixture are shown in Fig. 1. The top spectra (Fig. 1A) represent the starting material (in the absence of HOCl), and the bottom spectra (Fig. 1B) correspond to the organic extracts of plasma-

logens after reaction with 5 mM HOCl. The plasmalogen concentration was 2 mM. Untreated OOPC_{plasm} (left traces) gives two major peaks at m/z 772.6 and 794.6, corresponding to the neutral molecule cationized by H⁺ and Na⁺, respectively. These peaks disappear nearly completely upon treatment with a 2.5 molar excess of HOCl. New peaks arise in the low mass range at m/z 522.3 and 544.3, corresponding to the H⁺ and Na⁺ adducts of 1-lyso-2-oleoyl-*sn*-glycero-3-phosphocholine (2-O-1-LPC). The mass spectra of ODPC_{plasm} (right traces) change in a similar way by treatment with HOCl. The peaks at m/z 818.6 and 840.6, corresponding to the H⁺ and Na⁺ adducts of the starting material, disappear completely upon treatment with HOCl, and at m/z 568.3 and 590.3, peaks of 1-lyso-2-docosahexanoyl-*sn*-glycero-3-phosphocholine (2-D-1-LPC) appear concomitantly. The spectra in Fig. 1 also contain additional peaks at m/z 468.3 and 490.3, corresponding to the proton and sodium adducts of 1-M-2-LPC, and at m/z 760.6 and 782.6, corresponding to POPC. Both substances were added to the organic plasmalogen extracts as internal standards to allow a reliable quantitative evaluation of the reaction products.

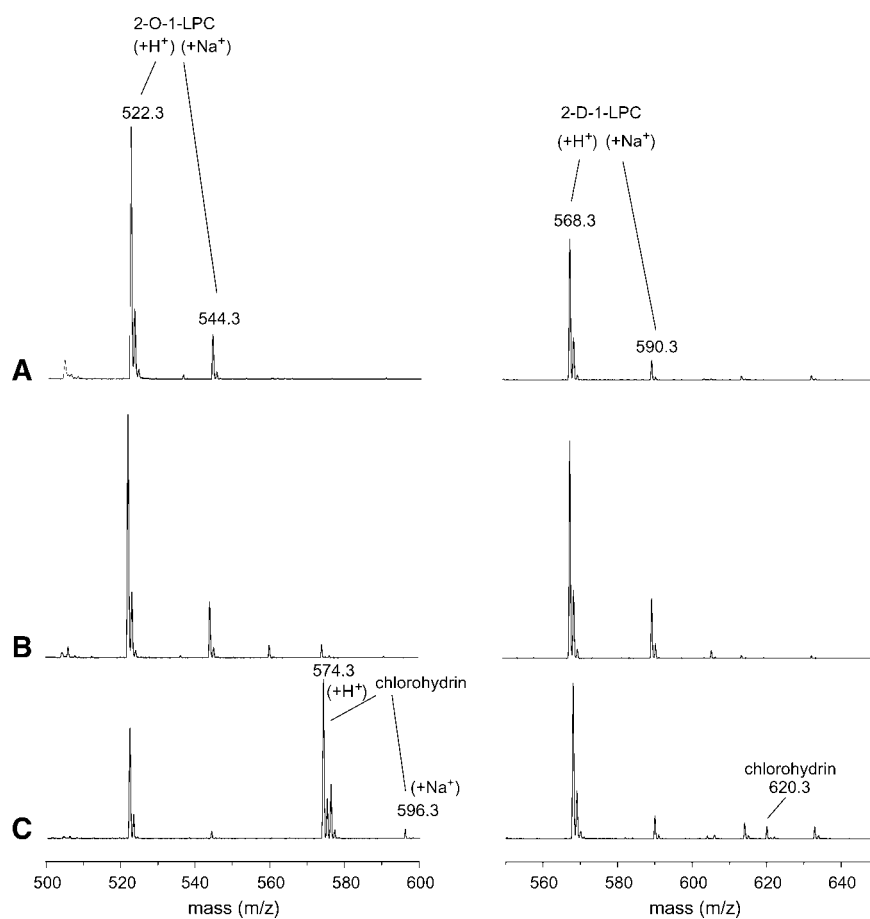


Fig. 4. Positive ion MALDI-TOF mass spectra of the chloroform phases of the organic extracts of plasmalogen glycerophosphocholines incubated with 2.5 mM HOCl (A), 5 mM HOCl (B), or 10 mM HOCl (C) for 1 h at room temperature. The plasmalogen concentration was 2 mM in all cases. Spectra at left correspond to OOPC_{plasm}, and spectra at right correspond to ODPC_{plasm}. Spectra were scaled according to the intensity of the 1-M-2-LPC standard, and the m/z values and peak assignments are indicated.

The aqueous extracts of both plasmalogens incubated with HOCl were also analyzed by MALDI-TOF MS (Fig. 2). New peaks appeared at m/z 258.1 and 280.1 in the HOCl-treated (10 mM) OOPC_{plasm} (Fig. 2B) and ODPC_{plasm} (Fig. 2C) samples, in contrast to the untreated controls (data not shown). These peaks correspond to the proton and sodium adducts of GPC. It is evident that the yield of GPC upon HOCl incubation of ODPC_{plasm} (Fig. 2C) exceeds that of OOPC_{plasm} (Fig. 2B). All other peaks in Fig. 2 are caused by the PNA matrix, as indicated by the spectrum of the pure PNA matrix (Fig. 2A). Of course, these data are not absolutely reliable, because matrix peak intensities are influenced by many other parameters. However, these data were confirmed by another independent method (³¹P NMR; see below).

To evaluate the relative contributions of 1-lyso-2-fatty acyl glycerophosphocholine lipids and GPC formed as a result of the incubation of HOCl with plasmalogens in more detail, products were analyzed in relation to the concentrations of HOCl in the incubation mixture (Fig. 3). Peaks of interest were referenced to the intensities of the internal standards [i.e., the sum of the intensities of the proton and sodium adducts of 1-myristoyl-2-lyso-*sn*-glycerophosphocholine (m/z 468.3 and 490.3) for 1-lyso-2-fatty

acyl glycerophosphocholines and the sum of the intensities of the proton and sodium adducts of 1-palmitoyl-2-oleoyl-*sn*-glycero-phosphocholine (m/z 760.6 and 782.6) for the plasmalogen glycerophosphocholines]. The most pronounced PNA matrix peak at m/z 229 served as a reference for the formation of GPC (Fig. 3B). Although not yet comprehensively established for PNA, this approach offers different advantages, particularly the fact that there is no need to add a reference compound.

Peaks of both plasmalogens decreased continuously with increasing HOCl concentrations. No plasmalogens were detected at HOCl concentrations $> 5 \times 10^{-3}$ mol/l. There were no significant reactivity differences between ODPC_{plasm} and OOPC_{plasm}. 1-Lyso-2-fatty acyl glycerophosphocholine lipids (2-D-1-LPC from ODPC_{plasm} and 2-O-1-LPC from OOPC_{plasm}) were clearly detected at 10^{-3} mol/l and greater HOCl concentrations. The highest yields of 2-D-1-LPC and 2-O-1-LPC were detected at 2.5×10^{-3} mol/l and 5×10^{-3} mol/l HOCl, respectively. Using still higher HOCl concentrations, the yields of both LPCs decreased continuously.

The formation of GPC was observed only at 5×10^{-3} mol/l and greater HOCl concentrations. A pronounced formation of GPC occurred only in the case of

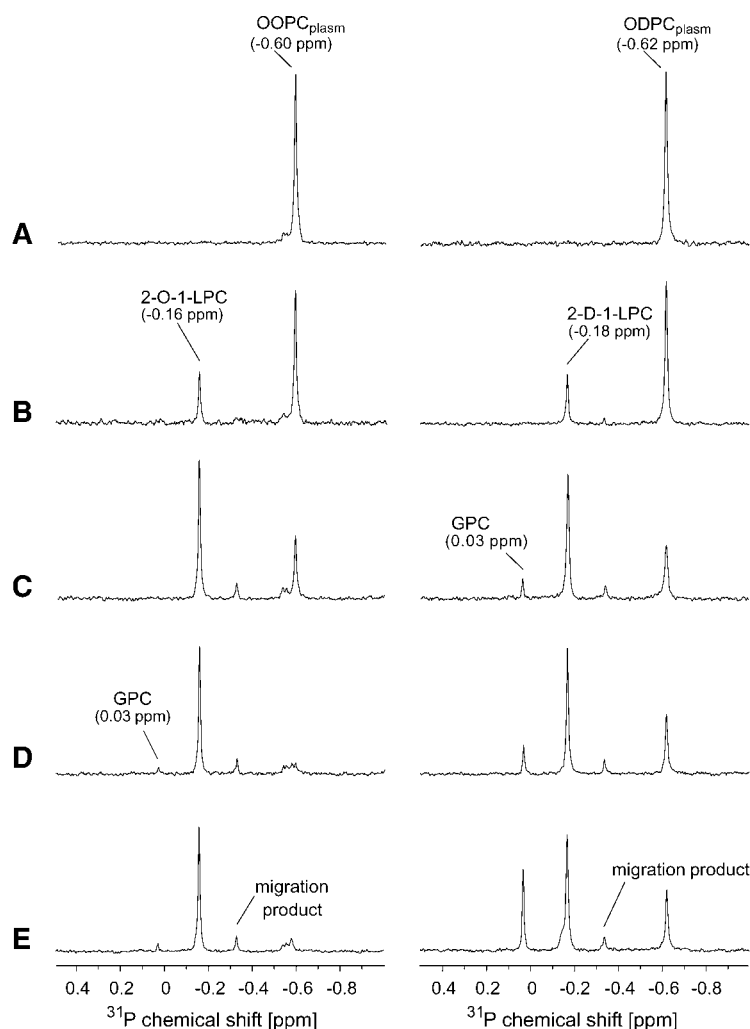


Fig. 5. ³¹P NMR spectra (242.88 MHz) of the combined organic and aqueous extracts of plasmalogen glycerophosphocholine after incubation with buffer (A) or 1 mM (B), 5 mM (C), 7.5 mM (D), or 10 mM (E) HOCl for 1 h at room temperature. The plasmalogen concentration was 2 mM in all cases. OOPC_{plasm} spectra are shown at left, and ODPC_{plasm} spectra are shown at right. Spectra were scaled according to the 1,2-dipalmitoyl-*sn*-glycero-3-phosphate standard resonance (peak outside the shown range at 3.15 ppm), and the peak assignment and chemical shifts are indicated. The signal-to-noise ratio differs slightly between the individual spectra because not exactly the same number of scans was accumulated in all spectra.

ODPC_{plasm} but not in the OOPC_{plasm} samples. This is not surprising, because it was already shown that phosphatidylcholine lipids with only one double bond under the influence of HOCl give much smaller yields of the 2-lyso-1-fatty acyl glycerophosphocholine lipids compared with higher unsaturated species (15, 16). One additional product was detected in the plasmalogen mass spectra at HOCl concentrations $> 5 \times 10^{-3}$ mol/l. This product corresponds to the monochlorohydrin derived from 2-O-1-LPC with peaks at m/z 574.3 and 596.3 for the proton and sodium adducts, respectively (Fig. 4, left traces). Using ODPC_{plasm} only traces of the corresponding chlorohydrin species were detected at m/z 620.3 for the proton adduct (Fig. 4, right traces).

Besides the plasmalogens discussed to this point, a third plasmalogen [1-O-1'-(Z)octadecenyl-2-arachidonoyl-*sn*-glycero-3-phosphocholine (OAPC_{plasm})] is still commercially available and was also used. The same incubation and quantification procedures were used to evaluate the relative contributions of 1-LPC and GPC formed from OAPC_{plasm} (data not shown). OAPC_{plasm} incubations with HOCl gave complementary results. No plasmalogens were detected at HOCl concentrations $> 5 \times 10^{-3}$ mol/l. LPC lipids were also clearly detected at 10^{-3} mol/l and greater HOCl concentrations. The formation of GPC from OAPC_{plasm} started at 5×10^{-3} mol/l HOCl. At 10^{-2} mol/l HOCl, the relative GPC moiety derived from OAPC_{plasm} was 1.01, corresponding to an average value of OOPC_{plasm} and ODPC_{plasm} (Fig. 3B).

Reaction products of plasmalogens subsequent to the reaction with HOCl were additionally analyzed by ^{31}P NMR spectroscopy. For this purpose, the aqueous and CHCl_3 phases were evaporated to dryness, combined, and redissolved in aqueous sodium cholate. This was done to have a suitable reference to the mass spectra for when the aqueous and CHCl_3 layers were investigated separately. The ^{31}P NMR spectra of OOPC_{plasm} (left traces) and ODPC_{plasm} (right traces) after incubation with different concentrations of HOCl are shown in Fig. 5. In Fig. 5A, the ^{31}P NMR spectra of both plasmalogen glycerophosphocholine lipids incubated with pure buffer in the absence of HOCl are shown as reference. The only peak appearing in both spectra represents the resonance of the plasmalogens (-0.60 and -0.62 ppm) and proves the absence of even small amounts of LPC and GPC.

NMR spectra of OOPC_{plasm} (left traces) and ODPC_{plasm} (right traces) after treatment with HOCl are shown in Fig. 5B–E). The intensities of the plasmalogen resonances decrease when increasing amounts of HOCl are used. Additional peaks corresponding to LPCs (2-O-1-LPC and 2-D-1-LPC) are detected at -0.16 and -0.18 ppm, respectively, in the presence of 1 mM HOCl (Fig. 5B). A further increase of the LPC resonance intensities was observed at 5 mM HOCl (Fig. 5C). Finally, at still higher HOCl concentrations (7.5 and 10 mM), the intensity of the LPCs decreases (Fig. 5D, E). One should note that a partial migration of the fatty acid residue from the *sn*-2 to the *sn*-1 position takes place in mixed detergent-phospholipid micelles (35). Thus, a second resonance of the correspond-

ing LPC isomer is detectable at -0.33 ppm but with much lower intensity. This has nothing to do with the HOCl effect but is caused by a methodological factor.

The incubation of ODPC_{plasm} with 5 mM HOCl (Fig. 5C) revealed one additional new resonance at 0.03 ppm, corresponding to GPC. The GPC peak increases more significantly at higher HOCl concentrations in the ODPC_{plasm} samples, whereas only traces of GPC are detected in the case OOPC_{plasm}. One should also note that some other resonances appear in the region of the starting material at the highest HOCl concentrations (~ -0.55 ppm). These resonances most likely contribute to chlorohydrins and epoxides of the used plasmalogen. Because the resolution of such very similar compounds is quite poor, no efforts were made to assign these resonances in more detail.

A quantitative evaluation of the data from ^{31}P NMR spectra is given in Fig. 6 using 0.5 mM 1,2-dipalmitoyl-

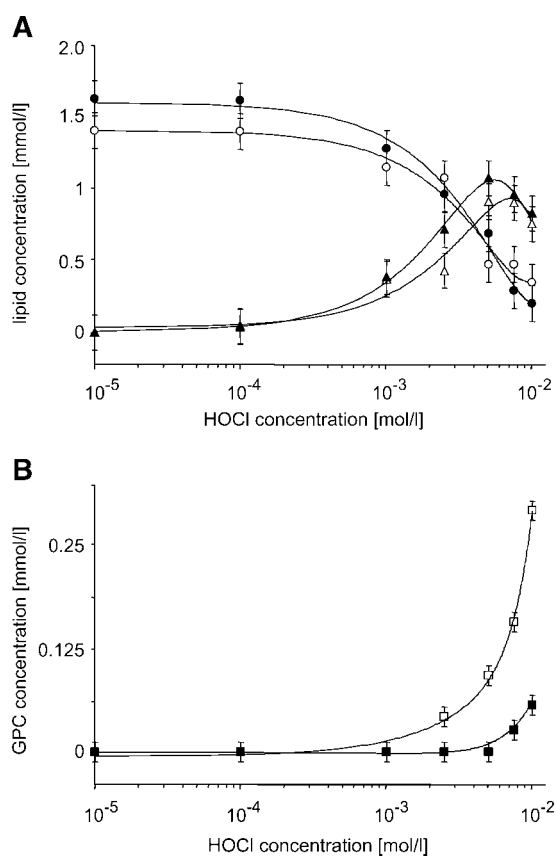


Fig. 6. Quantitative analysis of the integral peak intensities of the ^{31}P NMR spectra shown in Fig. 5: The absolute plasmalogen concentration according to the internal standard 1,2-dipalmitoyl-*sn*-glycero-3-phosphate (A) as well as the GPC concentration derived from ODPC_{plasm} (open squares) and OOPC_{plasm} (closed squares) (B) upon incubation with HOCl are shown. The concentrations of ODPC_{plasm} are indicated by open circles and those of OOPC_{plasm} by closed circles. The data for 2-D-1-LPC are indicated by open triangles and those of 2-O-1-LPC by closed triangles. Error bars represent SD of three independent measurements. The slight concentration differences between MALDI-TOF MS and ^{31}P NMR data are caused by methodological factors (i.e., varying detection sensitivities). The curved lines were not derived from a mathematical model but only represent spline curves to guide the eye.

sn-glycero-3-phosphate as an internal standard (^{31}P NMR chemical shift = 3.15 ppm; not shown in Fig. 5). With increasing HOCl concentrations, the concentrations of both plasmalogens decrease (Fig. 6A). The concentrations of 2-O-1-LPC and 2-D-1-LPC exhibit maxima at $\sim 5 \times 10^{-3}$ M HOCl, with a slightly higher value in the case of 2-O-1-LPC. A more pronounced formation of GPC from $\text{ODPC}_{\text{plasm}}$ compared with $\text{OOPC}_{\text{plasm}}$ is obvious at higher HOCl concentrations (Fig. 6B). Thus, NMR data indicate a comparable behavior to that shown by mass spectrometry.

DISCUSSION

The formation of α -chloro fatty aldehydes from plasmalogens subsequent to treatment with HOCl is well documented (13, 14). Here, we focused our attention on the fate of the other products of this reaction: on LPCs bearing an acyl chain in the *sn*-2 position. In Fig. 7, the proposed two-stage pathway of the reaction of HOCl with plasmalogens is shown. Our data clearly indicate that the vinyl-ether bond in both plasmalogen samples is the preferred target for HOCl. We were able to detect the formation of 2-O-1-LPC from $\text{OOPC}_{\text{plasm}}$ and 1-lyso-2-arachidonoyl-*sn*-glycero-3-phosphocholine from $\text{OAPC}_{\text{plasm}}$ as well as of 2-D-1-LPC from $\text{ODPC}_{\text{plasm}}$ at relatively low (10^{-3} M) HOCl concentrations by MALDI-TOF MS and ^{31}P NMR spectroscopy. Secondary reaction products resulting from both LPCs were detected only at 5 mM HOCl and higher concentrations. In the case of 2-O-1-LPC, the formation of the corresponding chlorohydrin derivative

dominates, whereas GPC is the preferred product from 2-D-1-LPC. This is in accordance with our previous observation that HOCl cleaves unsaturated fatty acyl chains from phosphatidylcholines. The yield of LPC increases considerably with the degree of unsaturation of the fatty acyl residues in the PC (15, 16). High amounts of LPCs were only formed from phospholipids containing arachidonoyl or docosahexaenoyl residues, and a possible mechanism to explain these findings has been proposed (15).

According to our results, GPC is formed from unsaturated plasmalogens (especially from higher unsaturated ones, such as $\text{OAPC}_{\text{plasm}}$ and $\text{ODPC}_{\text{plasm}}$) by sequential cleavage of the *sn*-1 and *sn*-2 residues. Weak chlorohydrin formation could be observed particularly in the $\text{OOPC}_{\text{plasm}}$ sample, but the generation of LPC lipids and glycerophosphocholine was considerably higher. Furthermore, we cannot exclude the existence of additional pathways. For instance, Thompson et al. (36) found upon photooxidation of plasmalogens a cleavage of the alkenyl-ether in the *sn*-1 position upon the formation of the lyso- and formyl-glycerophosphocholine. In contrast, oxidation along the fatty acid residue in the *sn*-2 position was also shown to occur under the influence of free radicals (37, 38). Such products are not observed in the presence of HOCl or are beyond our detection limits.

The sensitivity of the plasmalogen vinyl-ether bonds emphasizes their impact as physiological prime targets for HOCl and subsequent 1-lyso-2-fatty acyl glycerophosphocholine and GPC formation. In the majority of plasmalogens, the *sn*-1 position consists mainly of hexadecenyl or octadecenyl residues, whereas the *sn*-2 position is es-

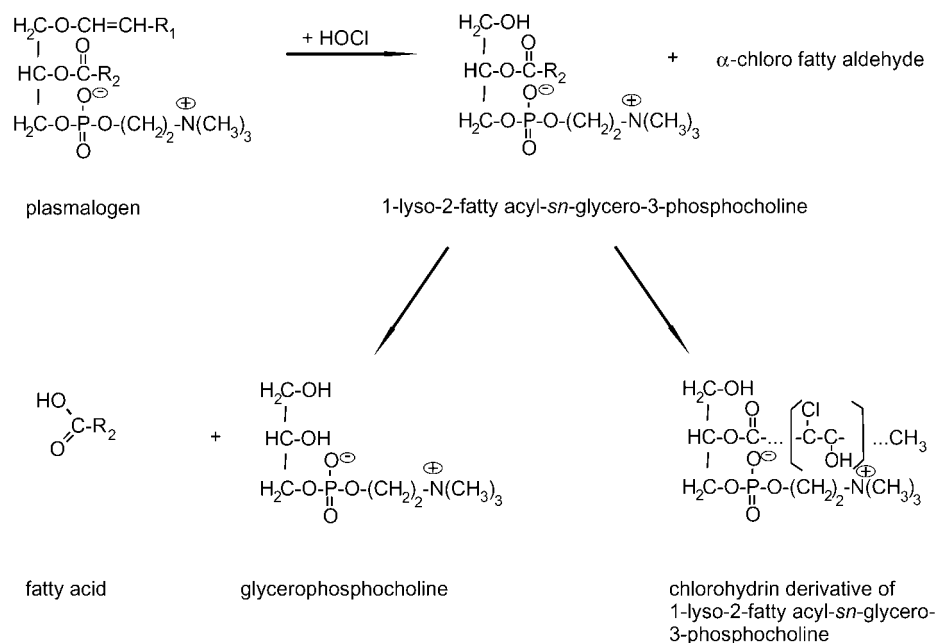


Fig. 7. Proposed two-stage process of the cleavage of the *sn*-1 plasmalogen glycerophosphocholine accompanied by the generation of 1-lyso-2-fatty acyl glycerophosphocholine and α -chloro fatty aldehydes. In the second step, a cleavage of the polyunsaturated fatty acid at the *sn*-2 position upon the formation of GPC, or alternatively upon the formation of chlorohydrins, takes place. R_1 , octadecenyl residue; R_2 , unsaturated acyl residue.

terified with polyunsaturated fatty acids and the head group is usually either ethanolamine or choline (1, 2). Different tissues and cell types contain significant amounts of plasmalogens. Brain possesses the highest content of plasmalogen glycerophosphoethanolamine, followed by spermatozoa, whereas heart has a higher content of plasmalogen glycerophosphocholine (3, 39). As glycerophosphoethanolamine contains an additional amino group that reacts readily with HOCl, plasmalogen glycerophosphocholine was used exclusively in this study to investigate the influence of the alkenyl ether at *sn*-1 and the fatty acid composition in the *sn*-2 position.

The reactive chlorinating species HOCl is known to be produced from H₂O₂ and Cl⁻ in the presence of MPO, an enzyme released by activated neutrophils and macrophages (6). Released MPO mediates, in part, the destruction of foreign organisms by producing toxic chlorinating species (40). In contrast, HOCl also targets host tissues and participates in cardiovascular pathophysiology (e.g., atherosclerosis) (18, 19) and other inflammatory diseases (e.g., rheumatoid arthritis) (41). Plasmalogens have been proposed not only as antioxidants but also as mediators of membrane dynamics and the storage of polyunsaturated fatty acids and lipid mediators (1, 2). Besides their involvement in plasmalogen-deficiency disorders, plasmalogens are also implicated in many diseases, including aging, Alzheimer's disease, heart diseases, and/or myocardial infarction (1, 2). Recently, HOCl has been shown to target the vinyl-ether bond of plasmalogen glycerophosphocholine, resulting in α -chloro fatty aldehydes and unsaturated 1-LPCs (17–19). LPC formation is known to be cytotoxic; thus, the proposed protective role of plasmalogens against oxidative damage potentially could be in competition with the damaging effects of the released LPC lipids (20). Therefore, following the fate of the 1-LPCs bearing an acyl chain at the *sn*-2 position is essential in understanding the putative role of plasmalogen glycerophospholipids as scavenger molecules.

The formation of glycerophosphocholine from plasmalogens under the influence of HOCl denotes a novel reaction pathway. Remarkably, GPC is generated in the absence of any phospholipase activities (i.e., exclusively under the influence of HOCl). Although GPC is unequivocally an important metabolite, there is yet no established correlation between increased GPC levels and different processes such as inflammation and ROS-mediated pathologies.

This study provides clear evidence that GPC formation occurs when ODPC_{plasm} is incubated with a slight excess of HOCl (e.g., 5 mM HOCl). This is close to physiologically relevant HOCl concentrations, although the in vivo stationary HOCl concentration is always near zero, because many potential targets are available. HOCl is produced continuously at inflammatory sites by MPO, and calculations revealed that 2–4 × 10⁶ leukocytes produce 100–140 μ mol of HOCl during 1 h (42). Furthermore, the same reaction would take place at reduced HOCl concentrations if the plasmalogen concentrations were decreased concomitantly. Thus, under inflammatory conditions, HOCl may be capable of triggering GPC generation throughout. In

the case of polyunsaturated plasmalogen, ODPC_{plasm} GPC is the main product besides 2-D-1-LPC at increased HOCl concentrations. These results confirm the previously underestimated role of plasmalogens as scavenger molecules in biological cells and tissues. GPC generation may be of particular relevance in animal spermatozoa (e.g., bull or boar), because these cells have very high plasmalogen moieties that consist primarily of docosahexanoic acid residues. ■

This work was supported by the Deutsche Forschungsgemeinschaft (Grants DFG GL 199/4 and Schi 476/5-1) and the German Ministry of Education and Research and the Bundesministerium für Bildung und Forschung (BMBF Grant 0313836).

REFERENCES

1. Nagan, N., and R. A. Zoeller. 2001. Plasmalogens: biosynthesis and functions. *Prog. Lipid Res.* **40**: 199–229.
2. Brites, P., H. R. Waterham, and R. J. A. Wanders. 2004. Functions and biosynthesis of plasmalogens in health and disease. *Biochim. Biophys. Acta.* **1636**: 219–231.
3. LeBig, J., C. Gey, R. Süß, J. Schiller, H.-J. Glander, and J. Arnhold. 2004. Analysis of the lipid composition of human and boar spermatozoa by MALDI-TOF mass spectrometry, thin layer chromatography and ³¹P NMR spectroscopy. *Comp. Biochem. Physiol.* **137**: 265–277.
4. Murphy, R. C. 2001. Free-radical-induced oxidation of arachidonoyl plasmalogen phospholipids: antioxidant mechanism and precursor pathway for bioactive eicosanoids. *Chem. Res. Toxicol.* **14**: 463–472.
5. Reiss, D., K. Beyer, and B. Engelmann. 1997. Delayed oxidative degradation of polyunsaturated diacyl phospholipids in the presence of plasmalogen phospholipids *in vitro*. *Biochem. J.* **323**: 807–814.
6. Klebanoff, S. J. 1991. Myeloperoxidase: occurrence and biological function. In *Peroxidases in Chemistry and Biology*. Vol. 1. J. Everse, K. E. Everse, and M. B. Grisham, editors. CRC Press, Boca Raton, FL. 1–35.
7. Winterbourn, C. C. 1985. Comparative reactivities of various biological compounds with myeloperoxidase-hydrogen peroxide-chloride, and similarity of oxidant to hypochlorite. *Biochim. Biophys. Acta.* **840**: 204–210.
8. Pattison, D. I., and M. J. Davies. 2001. Absolute rate constant for the reaction of hypochlorous acid with protein side chains and peptide bonds. *Chem. Res. Toxicol.* **14**: 1453–1464.
9. Hawkins, C. L., D. I. Pattison, and M. J. Davies. 2002. Hypochlorite-induced oxidation of amino acids, peptides and proteins. *Amino Acids.* **25**: 259–274.
10. Schiller, J., J. Arnhold, W. Gründer, and K. Arnold. 1994. The action of hypochlorous acid on polymeric components of cartilage. *Biol. Chem. Hoppe Seyler.* **375**: 167–172.
11. Prütz, W. A. 1996. Hypochlorous acid interactions with thiols, nucleotides, DNA, and other biological substrates. *Arch. Biochem. Biophys.* **332**: 110–120.
12. Arnhold, J., A. N. Osipov, H. Spalteholz, O. M. Panasenko, and J. Schiller. 2001. Effects of hypochlorous acid on unsaturated phosphatidylcholines. *Free Radic. Biol. Med.* **31**: 1111–1119.
13. Winterbourn, C. C., J. J. M. van den Berg, E. Roitman, and F. A. Kuypers. 1992. Chlorohydrin formation from unsaturated fatty acids reacted with hypochlorous acid. *Arch. Biochem. Biophys.* **296**: 547–555.
14. Van den Berg, J. J. M., C. C. Winterbourn, and F. A. Kuypers. 1993. Hypochlorous acid-mediated modification of cholesterol and phospholipids: analysis by gas chromatography-mass spectrometry. *J. Lipid Res.* **34**: 2005–2012.
15. Arnhold, J., A. N. Osipov, H. Spalteholz, O. M. Panasenko, and J. Schiller. 2002. Formation of lysophospholipids from unsaturated phosphatidylcholines under the influence of hypochlorous acid. *Biochim. Biophys. Acta.* **1572**: 91–100.
16. Panasenko, O. M., J. Schiller, H. Spalteholz, and J. Arnhold. 2003. Myeloperoxidase-induced formation of chlorohydrins and lysophos-

- pholipids from unsaturated phosphatidylcholines. *Free Radic. Biol. Med.* **34**: 553–562.
17. Marsche, G., R. Heller, G. Fauler, A. Kovacevic, A. Nizskowski, W. Graier, W. Sattler, and E. Malle. 2004. 2-Chlorohexadecanal derived from hypochlorite-modified high-density lipoprotein-associated plasmalogen is a natural inhibitor of endothelial nitric oxide biosynthesis. *Arterioscler. Thromb. Vasc. Biol.* **24**: 2302–2306.
 18. Thukkani, A. K., J. McHowat, F-F. Hsu, M-L. Brennan, S. L. Hazen, and D. A. Ford. 2003. Identification of chloro fatty aldehydes and unsaturated lysophosphatidylcholine molecular species in human atherosclerotic lesions. *Circulation.* **108**: 3128–3133.
 19. Thukkani, A. K., F-F. Hsu, J. R. Crowley, R. B. Wysolmerski, C. J. Albert, and D. A. Ford. 2002. Reactive chlorinating species produced during neutrophil activation target tissue plasmalogens. *J. Biol. Chem.* **277**: 3842–3849.
 20. Zhou, L., M. Shi, Z. Guo, W. Brisbow, R. Hoover, and H. Yang. 2006. Different cytotoxic injuries induced by lysophosphatidylcholine and 7-ketocholesterol in mouse endothelial cells. *Endothelium.* **13**: 213–226.
 21. Messner, M. C., C. J. Albert, F-F. Hsu, and D. A. Ford. 2006. Selective plasmenylcholine oxidation by hypochlorous acid: formation of lysophosphatidylcholine chlorohydrins. *Chem. Phys. Lipids.* **144**: 34–44.
 22. Wildsmith, K. R., C. J. Albert, D. S. Anbukumar, and D. A. Ford. 2006. Metabolism of myeloperoxidase-derived 2-chlorohexadecanal. *J. Biol. Chem.* **281**: 16849–16860.
 23. Thukkani, A. K., C. J. Albert, K. R. Wildsmith, M. C. Messner, B. D. Martinson, F-F. Hsu, and D. A. Ford. 2003. Myeloperoxidase-derived reactive chlorinating species from human monocytes target plasmalogens in low density lipoprotein. *J. Biol. Chem.* **278**: 36365–36372.
 24. Malle, E., G. Marsche, U. Panzenboeck, and W. Sattler. 2005. Myeloperoxidase-mediated oxidation of high-density lipoproteins: fingerprints of newly recognized potential proatherogenic lipoproteins. *Arch. Biochem. Biophys.* **445**: 245–255.
 25. Morris, J. C. 1966. Acid ionization constant of HOCl from 5 to 35 degrees. *J. Phys. Chem.* **70**: 133–140.
 26. Bligh, E. G., and W. J. Dyer. 1959. A rapid method of total lipid extraction and purification. *Can. J. Biochem. Physiol.* **37**: 911–917.
 27. Schiller, J., and K. Arnold. 2000. Mass spectrometry in structural biology. In *Encyclopedia of Analytical Chemistry*. R. A. Meyers, editor. Wiley, Chichester, UK. 559–585.
 28. Schiller, J., R. Süß, J. Arnhold, B. Fuchs, J. Leßig, M. Müller, M. Petković, H. Spalteholz, O. Zschörnig, and K. Arnold. 2004. Matrix-assisted laser desorption and ionization time-of-flight (MALDI-TOF) mass spectrometry in lipid and phospho-lipid research. *Prog. Lipid Res.* **43**: 443–478.
 29. Benard, S., J. Arnhold, M. Lehnert, J. Schiller, and K. Arnold. 1999. Experiments towards quantification of saturated and polyunsaturated diacylglycerols by matrix-assisted laser desorption and ionization time-of-flight mass spectrometry. *Chem. Phys. Lipids.* **100**: 115–125.
 30. Asbury, G. R., K. Al-Saad, W. F. Siems, R. M. Hannan, and H. H. Hill. 1999. Analysis of triacylglycerols and whole oils by matrix-assisted laser desorption/ionization time of flight mass spectrometry. *J. Am. Soc. Mass Spectrom.* **10**: 983–991.
 31. Estrada, R., and M. C. Yappert. 2004. Alternative approaches for the detection of various phospholipid classes by matrix-assisted laser desorption/ionization time-of-flight mass spectrometry. *J. Mass Spectrom.* **39**: 412–422.
 32. Pearce, J. M., and R. A. Komoroski. 2000. Analysis of phospholipid molecular species in brain by ³¹P NMR spectroscopy. *Magn. Reson. Med.* **44**: 215–223.
 33. London, E., and G. W. Feigenson. 1979. Phosphorus NMR analysis of phospho-lipids in detergents. *J. Lipid Res.* **20**: 408–412.
 34. Schiller, J., and K. Arnold. 2002. Application of high resolution ³¹P NMR spectroscopy to the characterization of the phospholipid composition of tissues and body fluids—a methodological review. *Med. Sci. Monit.* **8**: 205–222.
 35. Plückthun, A., and E. A. Dennis. 1982. Acyl and phosphoryl migration in lysophospholipids: importance in phospholipid synthesis and phospholipase specificity. *Biochemistry.* **21**: 1743–1750.
 36. Thompson, D. H., H. D. Inerowicz, J. Grove, and T. Sarna. 2003. Structural characterization of plasmenylcholine photooxidation products. *Photochem. Photobiol.* **78**: 323–330.
 37. Zemski Berry, K. A., and R. C. Murphy. 2005. Free radical oxidation of plasmalogen glycerophosphocholine containing esterified docosahexaenoic acid: structure determination by mass spectrometry. *Antioxid. Redox Signal.* **7**: 157–169.
 38. Khaselev, N., and R. C. Murphy. 2000. Peroxidation of arachidonate containing plasmenyl glycerophosphocholine: facile oxidation of esterified arachidonate at carbon-5. *Free Radic. Biol. Med.* **29**: 620–632.
 39. Diagne, A., J. Fauvel, M. Record, H. Chap, and L. Douste-Blazy. 1984. Studies on ether phospholipids. II. Comparative composition of various tissues from human, rat and guinea pig. *Biochim. Biophys. Acta.* **793**: 221–231.
 40. Klebanoff, S. J., A. M. Waltersdorff, and H. Rosen. 1984. Antimicrobial activity of myeloperoxidase. *Methods. Enzymol.* **105**: 399–403.
 41. Fuchs, B., J. Schiller, U. Wagner, H. Häntzschel, and K. Arnold. 2005. The phosphatidylcholine/lysophosphatidylcholine ratio in human plasma is an indicator of the severity of rheumatoid arthritis: investigations by ³¹P NMR and MALDI-TOF MS. *Clin. Biochem.* **38**: 925–933.
 42. Weiss, S. J., R. Klein, A. Slivka, and M. Wei. 1982. Chlorination of taurine by human neutrophils: evidence for hypochlorous acid generation. *J. Clin. Invest.* **70**: 598–607.